

**FRACTURE AND FATIGUE BEHAVIOR OF WC-Co
AND WC-CoNi CEMENTED CARBIDES**

J. M. Tarragó^{1,2*}, J. J. Roa^{1,2}, V. Valle¹, J. M. Marshall³, L. Llanes^{1,2}

¹ CIEFMA, Departament de Ciència dels Materials i Enginyeria Metal·lúrgica, Universitat Politècnica de Catalunya, ETSEIB, Avda. Diagonal 647, 08028 Barcelona, Spain

* e-mail: jose.maria.tarrago@upc.edu

² CRnE, Centre de Recerca en Nanoenginyeria, Universitat Politècnica de Catalunya, Barcelona 08028, Spain

³ Sandvik Hyperion, Coventry CV4 0XG, UK

ABSTRACT

The fracture and fatigue characteristics of several cemented carbide grades are investigated as a function of their microstructure. In doing so, the influence of binder chemical nature and content (Co and 76_{wt%}Co-24_{wt%}Ni), as well as carbide grain size on hardness, flexural strength, fracture toughness and fatigue crack growth (FCG) behavior is evaluated. Mechanical testing is combined with a detailed inspection of crack-microstructure interaction, by means of scanning electron microscopy, in order to evaluate crack-path tortuosity and to discern fracture and fatigue micromechanisms within the metallic binder. Results show that CoNi-base hardmetals exhibit slightly lower hardness but higher toughness values than Co-base grades. Meanwhile, flexural strength is found to be rather independent of the binder chemical nature. Regarding FCG behavior, experimental results indicate that: (1) FCG threshold (K_{th}) values for coarse-grained grades are higher than those measured for the medium-grained ones; and (2) fatigue sensitivity levels exhibited by CoNi- and Co-base cemented carbides, for a given binder mean free path, are similar. These findings are rationalized on the basis of the increasing relevance of crack deflection mechanisms as microstructure gets coarser and the evidence of similar fatigue degradation phenomena within the binder independent of its chemical nature, respectively.

KEYWORDS: Fatigue crack growth, cemented carbides, crack deflection, fractography, alternative binders.

1. INTRODUCTION

Cobalt is the most widely used binder metal in cemented carbides because the excellent interface properties exhibited by the WC-Co system [1]. However, one of the major trends in hardmetals industry is focused in finding new binder phases to replace cobalt [2,3]. Main reasons for this are the toxicity of cobalt, the improvement of the performance under severe working conditions, the requirement to find simpler manufacturing techniques and cobalt price increase and fluctuation [3,4]. Among the iron group metals, Nickel and Iron binders have attracted considerable attention as substitutes for Cobalt because their good wettability with WC as well as their capability for being manufactured into full dense compounds. However, mechanical properties of Ni- and Fe-base hardmetals tend to be inferior to those of Co-base grades, and the carbon content control becomes more complicated [3]. On the other hand, it has been demonstrated that the corrosion and oxidation resistance of cemented carbides is improved by replacing Co binders by Ni ones [5]. Furthermore, the mechanical properties of Ni-base hardmetals may be improved by alloying the binder metal with other elements such as Si, Mo or Cr (e.g. [5–7]) via solid solution. Accordingly, understanding the microstructure-property relationship of hardmetals constituted by alternative binders is critical for its proper development.

Fatigue is a relevant service degradation phenomenon in hardmetals and is associated with premature and unexpected failure [8]. Although the earliest information on fatigue of cemented carbides dates from 1941 [9], the more relevant scientific and technical advances on this field are concentrated in the last two decades. Among them, it is noteworthy the findings reported by Sockel's [10–13] and Llanes's [14–16] groups, developed following different testing approaches: applied stress – fatigue life (S-N curves) and Fatigue Crack Growth (FCG) tests, respectively. Schleinkofer and co-workers documented a strong strength degradation of cemented carbides under cyclic loads mainly related to fatigue degradation localized in the ductile binder phase [10–12]. Furthermore, through their systematic work, they were able to identify the subcritical crack

growth of preexisting flaws as the controlling stage for fatigue failure in these materials [10–13]. On the other hand, Torres and co-workers proposed the FCG threshold as the effective toughness under cyclic loading [14]. Moreover, they pointed out that fatigue sensitivity of hardmetals is significantly dependent on microstructure, according to the compromising role played by the binder as the main toughening and fatigue susceptible agent in cemented carbides [15]. This fatigue degradation ascribed to the metallic phase, also observed from the experimental S-N data published by Sailer and co-workers [17], has been rationalized - at least partly - on the basis of the cyclic strain-induced fcc to hcp phase transformation within the Co binder [10,11]. Consequently, the use of alternative binders with different chemical nature (e.g. Ni-containing ones) has been continuously proposed as an option for decreasing the fatigue sensitivity of cemented carbides. Following the above ideas, it is the main goal of this investigation to evaluate the influence of binder chemical nature and content (Co and 76_{wt%}Co-24_{wt%}Ni) on the fracture and fatigue behavior of cemented carbides. Within this context, a second objective is to document and analyze the influence of microstructural coarsening on the FCG behavior of the referred materials. This information is also relevant from a design viewpoint, as literature data combining fracture and fatigue characteristics for these materials are mainly concentrated on relatively finer-grained grades.

Symbols and definitions a_{cr} Critical half-flaw size da/dN FCG rate K_{Ic} Plain-strain fracture toughness K_{max} Maximum stress intensity factor K_{th} Fatigue crack growth threshold ΔK Stress intensity factor range R_L Crack linear roughness α_m Crack weighted mean deflected angle α_n Deflected angle of a crack chord L_T Crack length L_n Length of a crack chord σ_f Fatigue limit σ_r Flexural strength

2. MATERIALS AND METHODS

The investigated materials were WC-Co and WC-CoNi cemented carbides supplied by Sandvik Hyperion. Eight grades corresponding to different combinations of binder chemical nature, binder content and carbide grain size were studied. The designations and key microstructural parameters: binder content (%_{wt} binder), mean grain size (d_{WC}), carbide contiguity (C_{WC}), and binder mean free path (λ_{binder}) are listed in **Table 1**. Mean grain size was measured following the linear intercept method, using field emission scanning electron microscopy (FE-SEM) micrographs taken in a JEOL-7001F unit. Carbide contiguity and binder mean free path were deduced from best-fit equations, attained after compilation and analysis of data published in the literature (e.g. [18,19]), on the basis of empirical relationships given by Roebuck and Almond [19] but extending them to include carbide size influence [20,21].

Mechanical characterization for all the materials investigated included hardness (HV30), flexural strength (σ_f), fracture toughness (K_{Ic}) and fatigue crack growth (FCG) parameters. Additionally, fatigue limit (corresponding to infinite fatigue life of 10^7 cycles) was determined for four selected hardmetal grades. Hardness was measured using a Vickers diamond pyramidal indenter and applying a load of 294N. In all the others cases, testing was conducted using a four-point bending fully articulated test jig with inner and outer spans of 20 and 40 mm respectively. Flexural strength and fatigue life tests were performed on an Instron 8511 servohydraulic machine and on a RUMUL resonant testing machine, respectively. In both cases, at least 15 specimens of 45x4x3 mm dimensions were tested per grade. The surface which was later subjected to the maximum tensile loads was polished to mirror-like finish and the edges were chamfered to reduce their effect as stress raisers. Flexural strength results were analyzed using Weibull statistics and fatigue life tests were conducted following an up-and-down methodology for a load ratio (R) of 0.1. Fracture toughness and FCG parameters were determined using 45x10x5 mm single edge pre-cracked notch beam (SEPNB) specimens with a notch length-to-specimen width ratio of 0.3. Compressive cyclic loads were induced in the notched beams to nucleate a sharp crack and details may be found

elsewhere [22]. The sides of SEPNB specimens were polished to follow stable crack growth using a high-resolution confocal microscope. Fracture toughness was determined by testing SEPNB specimens to failure at stress-intensity factor load rates of about $2 \text{ MPa}\sqrt{\text{m/s}}$. FCG behavior was assessed for two different R values, 0.1 and 0.5, using a RUMUL resonant testing machine at load frequencies around 150 Hz. Detailed inspection of crack-microstructure interaction as well as the corresponding fractographic analysis on broken specimens were carried out by means of FE-SEM.

3. RESULTS AND DISCUSSION

Hardness, Flexural Strength and Fracture Toughness

Hardness, flexural strength and fracture toughness of the investigated materials are listed in **Table 2**. As previously reported [5], experimental results indicate that CoNi-base hardmetals exhibit slightly lower hardness and higher toughness values than Co-based grades (**Figure 1**). Main reason behind this finding is the higher stacking fault energy of Ni that results in lower hardening rates [3]; thus, Co-Ni binder alloys exhibit lower strength but higher ductility than cobalt [23,24]. On the other hand, a clear influence of the binder chemical nature on the flexural strength was not evidenced. Experimental data dispersion evidenced for this parameter is fairly small for all studied materials; and accordingly, the corresponding Weibull analysis yields quite high values, indicative of an expected outstanding reliability from a structural viewpoint.

Fatigue Crack Growth

FCG rate versus the stress intensity factor range (ΔK) and the maximum stress intensity factor (K_{max}) plots, including data for the two studied load ratios (0.1 and 0.5), are shown in Figures 2 and 3 for the studied Co- and CoNi-base cemented carbides, respectively. FCG thresholds (K_{th}), defined at crack growth rates of 10^{-6} mm/cycle, were attained following a decremental loading sequence. As previously reported, studied hardmetals exhibit FCG at ΔK values much lower than corresponding fracture toughness levels, and large-power dependences between FCG rates (da/dM) and ΔK . Furthermore, load ratio effects are reduced when plotting FCG rates against K_{max} , pointing out the predominance of static over cyclic failure modes [15,25,26].

Table 3 shows the determined fatigue threshold and fatigue sensitivity [$1-(K_{th}/K_{Ic})$] levels for the studied hardmetal grades. FCG parameters are quite similar for grades with alike microstructures (i.e. carbide size and binder content), but different binder chemical nature. On the other hand, coarse-grained materials exhibit higher fatigue threshold values than those determined for medium-

grained ones. This improvement is related to a more effective crack-deflection (e.g. **Figure 4**), as microstructure gets coarser, which remains operative under cyclic loading, i.e. toughening discerned under monotonic loading is not inhibited or degraded by fatigue. In **Figure 5** the FCG threshold is plotted as a function of the carbide mean grain size for the investigated hardmetals, together with the data reported in previous studies for a load ratio of 0.1 [15,21,26] and grades whose binder content ranges from 3 to 18 %_{wt}. It is found that the fatigue threshold (K_{th}) correlates linearly with the carbide mean grain size (d_{WC}) according to:

$$K_{th} = 5.75 + 1.27d_{WC} \quad (1)$$

with a coefficient of determination (R^2) of 0.91.

In order to better understand the influence of carbide mean grain size on the crack deflection mechanism, the geometry of the fatigue crack path was characterized by measuring two parameters (**Figure 6**):

- Crack linear roughness (R_L) [27] given by

$$R_L = \frac{\sum_1^n L_n}{L_T} \quad (2)$$

- and crack weighted mean deflected angle (α_m), defined as

$$\alpha_m = \frac{\sum_1^n L_n * \alpha_n}{\sum_1^n L_n} \quad (3)$$

where L_n is the length of crack segments, α_n is the angle between the segments and the straight line from the start to the end of the crack and L_T is the total length of this line. The analyzed fatigue crack growth paths corresponded to regions where cracks were propagated at applied K_{max} values slightly above the FCG threshold (i.e. between 7.5 and 10 MPa \sqrt{m}), and over 200 crack segments were measured per grade. The R_L and α_m values obtained for the investigated grades are plotted against the mean grain size in **Figure 7**. The quantified fracture parameters exhibit a linear dependence on the carbide mean grain size with R^2 coefficients of 0.84 and 0.85 for α_m and R_L , respectively. These results proof that higher fatigue threshold levels obtained for coarse-grained

cemented carbides are associated with an increase of the crack deflection angle, which results in a larger effective distance covered by the crack.

Fatigue crack growth threshold – Fatigue limit correlation

Based on the assumption that subcritical crack growth is the controlling stage for fatigue failure in cemented carbides [10–13], Torres and co-workers proposed and successfully validated a FCG threshold – fatigue limit correlation for WC-Co hardmetals within the Linear Elastic Fracture Mechanics (LEFM) framework [14,16]. In doing so, they defined the FCG threshold as the effective toughness under the application of cyclic loads for an infinite life approach. Thus, the fatigue limit (σ_f) can be deduced from the stress intensity factor threshold of a small non-propagating crack emanating from a defect of critical size, $2a_{cr}$, through a relationship of type:

$$\sigma_f = Y * \frac{K_{th}}{\sqrt{a_{cr}}} \quad (4)$$

where Y is a crack geometry factor. Accordingly, fatigue limit (σ_f) values can be estimated from the relation given by the expression (5) under the assumption that failure-controlling flaws under the application of monotonic and cyclic loadings have similar size, geometry and distribution.

$$\frac{\sigma_f}{\sigma_r} = \frac{K_{th}}{K_{Ic}} \quad (5)$$

Aiming to validate the above relationship, fatigue limit values were experimentally determined, following an up-and-down load (stair-case) methodology, for four of the hardmetal grades under consideration: 11CoM, 10CoC, 15CoC and 15CoNiC grades (**Figure 8**). An excellent agreement is obtained between predicted - using relationship (5) - and experimentally determined fatigue limits (**Table IV**), validating then the referred FCG threshold – fatigue limit correlation. A detailed FESEM fractographic examination of samples broken under cyclic loads pointed out critical defects of similar nature and geometry to those observed in failed specimens tested under monotonic loading.

However, under the application of cyclic loads these defects act as starting locations for subcritical crack growth until they reach a critical size where unstable fracture takes place (**Figure 9**).

Fatigue sensitivity

Llanes et al. [15] investigated the dependence of fatigue sensitivity of WC-Co hardmetals as a function of binder mean free path and applied load ratio. The trends proposed in Ref. [15] are plotted in **Figure 10**, together with the fatigue sensitivity exhibited by the studied cemented carbides. For $R = 0.1$ trend taken from Llanes et al.'s work is also updated with the results obtained in this investigation for the studied WC-Co and WC-CoNi cemented carbides. It is clear that coarse-grained cemented carbides here investigated exhibit lower fatigue sensitivity than expected for WC-Co grades with alike binder mean free path. Once again, the higher relevance of crack deflection mechanism as microstructure gets coarser, should here be recalled for rationalizing such finding [26]. Meanwhile, fatigue sensitivity of Co- and CoNi-base cemented carbides follow similar trends. These results are in agreement with a recent study on the FCG of a WC-Ni hardmetal by the authors, where similar fatigue sensitivity values for Nickel and Cobalt based cemented carbides was reported [28]. It would point out that degradation susceptibility under fatigue of toughening mechanisms operative in the ductile Co and CoNi binders under monotonic loading should be similar. Very interesting is that it seems to apply, even though the nature of the binder plastic deformation mechanisms shift from fcc-hcp transformation to slip plus twinning, as the Ni content in the binder increases [29]. In this regard, it is interesting to highlight that plastic deformation mechanisms in the Ni binder include slip and twinning [29,30], also discerned in the Co-base binders, but not stress-induced phase transformation, as it is the case in WC-Co grades.

Indirect evidence for the above ideas may be gathered from detailed inspection of both crack-microstructure interaction as well as fractographic features. Regarding the former, a crystallographic stable crack growth path within the binder has been evidenced independent of the binder chemical

nature (e.g. **Figure 4**). Concerning the latter, similar crystallographic step-like features are observed within the binder in the stable crack growth region for studied Co- and CoNi- base cemented carbides (**Figure 11**). Although the existence of these crystallographic-like paths is documented (e.g. [15,26,28,31-33]), the nature of the fatigue micromechanisms associated with them is not still clear.

4. CONCLUSIONS

The fracture and fatigue characteristics of eight microstructurally different WC-Co and WC-CoNi cemented carbides were investigated. Based on the obtained data the following conclusions may be drawn:

1. Experimental results indicate that hardness decreases and fracture toughness increases as the binder chemical nature is shifted from cobalt to cobalt/nickel. On the other hand, within the composition and microstructural range of hardmetal grades studied, flexural strength did not show any relevant influence on binder chemical nature.
2. FCG threshold of cemented carbides linearly rises when increasing carbide mean grain size, due to a more effective action of the crack deflection mechanism. Therefore, coarse-grained hardmetals are found to be less fatigue sensitive than finer-graded with similar binder mean free path.
3. FCG threshold and fatigue sensitivity are quite similar for grades with alike microstructures (i.e. carbide size and binder content), but different binder chemical nature. This negligible influence of binder chemical nature points then out that ductile Co and CoNi binders exhibit similar degradation susceptibility under fatigue of toughening mechanisms operative under monotonic loading. Such statement is supported by the faceted and crystallographic features evidenced, for all the hardmetal grades studied, in crack growth paths as well as in fracture surfaces corresponding to stable crack growth under cyclic loading.

ACKNOWLEDGEMENTS

This work was financially supported by the Spanish Ministerio de Economía y Competitividad (Grant MAT2012-34602). Additionally, J.M. Tarragó acknowledges the Ph.D. scholarship received from the collaborative Industry-University program between Sandvik Hyperion and Universitat Politècnica de Catalunya.

BIBLIOGRAPHY

- [1] Exner HE. Physical and chemical nature of cemented carbides. *Int Met Rev* 1979;24:149–73.
- [2] Prakash LJ. Developments in tungsten carbide-cobalt cemented carbides. *Int Powder Metall Direc* 2008;131–48.
- [3] Norgren S, Garcia J, Blomqvist A, Yin L. Global trends in the hard metals industry. In: . *Proceedings 18th Plansee Seminar, Reutte: Plansee Group; 2013, [OS 3/1–29]*
- [4] Brookes K. There's more to hard materials than tungsten carbide alone. *Metal Powder Rep* 2011;66:36–45.
- [5] Tracey VA. Nickel in hardmetals. *Int J Refract Met Hard Mat* 1992;11:137–49.
- [6] Correa EO, Santos JN, Klein a. N. Microstructure and mechanical properties of WC Ni–Si based cemented carbides developed by powder metallurgy. *Int J Refract Met Hard Mat* 2010;28:572–5.
- [7] Lin N, Wu CH, He YH, Zhang DF. Effect of Mo and Co additions on the microstructure and properties of WC–TiC–Ni cemented carbides. *Int J Refract Met Hard Mat* 2012;30:107–13.
- [8] Llanes L, Anglada M, Torres Y. Fatigue of cemented carbides. In: Sarin VK, Mari D, Llanes L, editors. *Comprehensive Hard Materials*, Elsevier; 2014, 345–62.
- [9] Dawihl W. Die wissenschaftlichen und technischen Grundlagen der pulvermetallurgie und ihrer anwendungsbereiche. *Stahl U. Eisen* 1941;61:909–19.
- [10] Schleinkofer U, Sockel HG, Gortig K, Heinrich W. Microstructural processes during subcritical crack growth in hard metals and cermets under cyclic loads. *Mat Sci Eng A* 1996;209:103–10.
- [11] Schleinkofer U, Sockel HG, Gortig K, Heinrich W. Fatigue of hard metals and cermets. *Mat Sci Eng A* 1996;209:313–7.
- [12] Schleinkofer U, Sockel HG, Görtig K, Heinrich W. Fatigue of hard metals and cermets - New results and a better understanding. *Int J Refract Met Hard Mat* 1997;15:103–12.
- [13] Kursawe S, Pott P, Sockel HG, Heinrich W, Wolf M. On the influence of binder content and binder composition on the mechanical properties of hardmetals. *Int J Refract Met Hard Mat* 2001;19:335–40.
- [14] Torres Y, Anglada M, Llanes L. Fatigue mechanics of WC–Co cemented carbides. *Int J Refract Met Hard Mat* 2001;19:341–8
- [15] Llanes L, Torres Y, Anglada M. On the fatigue crack growth behavior of WC–Co cemented carbides: kinetics description, microstructural effects and fatigue sensitivity. *Acta Mater* 2002;50:2381–93.
- [16] Torres Y, Anglada M, Llanes L. Fatigue limit - fatigue crack growth threshold correlation for hardmetals: influence of microstructure. In: Blom AF, editor. *Proceedings of the 8th International Fatigue Congress, Stockholm: 2002.*

- [17] Sailer T, Herr M, Sockel H-G, Schulte R, Feld H, Prakash LJ. Microstructure and mechanical properties of ultrafine-grained hardmetals. *Int J Refract Met Hard Mat* 2001;19:553–9.
- [18] Viswanadham RK, Sun TS, Drake EF, Peck J. Quantitative fractography of WC-Co cermets by Auger spectroscopy. *J Mat Sci* 1981;16:1029–38.
- [19] Roebuck B, Almond EA. Deformation and fracture processes and the physical metallurgy of WC-Co hardmetals. *Int Mat Rev* 1988;33:90–110.
- [20] Torres Y. Comportamiento a fractura y fatiga de carburos cementados WC-Co. PhD Thesis, Universitat Politècnica de Catalunya, 2002.
- [21] Coureaux D. Comportamiento mecánico de carburos cementados WC-Co: Influencia de la microestructura en la resistencia a la fractura, la sensibilidad a la fatiga y la tolerancia al daño inducido bajo sollicitaciones de contacto. PhD Thesis, Universitat Politècnica de Catalunya, 2012.
- [22] Torres Y, Casellas D, Anglada M, Llanes L. Fracture toughness evaluation of hardmetals: influence of testing procedure. *Int J Refract Met Hard Mat* 2001;19:27–34.
- [23] Penrice TW. Some characteristics of the binder phase in cemented carbides. *Int J Refract Met Hard Mat* 1997;15:113–21.
- [24] Almond EA, Roebuck B. Identification of optimum binder phase compositions for improved WC hard metals. *Mat Sci Eng A* 1988;105/106:237–48.
- [25] Fry PR, Garret GG. Fatigue crack growth behaviour of tungsten carbide-cobalt hardmetals. *J Mat Sci* 1988;23:2325–38.
- [26] Torres Y, Tarrago JM, Tarrés E, Roebuck B, Chan P, James M, et al. Fracture and fatigue of rock bit cemented carbides: mechanics and mechanisms of crack growth resistance under monotonic and cyclic loading. *Int J Refract Met Hard Mat* 2014;45:179-188.
- [27] Sigl LS, Exner HE. Experimental study of the mechanics of fracture in WC-Co alloys. *Metal Mater Trans A* 1987;18A:1299–308.
- [28] Tarragó JM, Ferrari C, Reig B, Coureaux D, Schneider L, Llanes L. Fatigue behavior of a WC-Ni Cemented Carbide. *Proceedings 18th Plansee Seminar. Reutte, Austria: Plansee SE; 2013 [HM103/1-9]*
- [29] Drake EF, Krawitz AD. Fatigue damage in a WC-Nickel cemented carbide composite. *Metal Mater Trans A* 1981;12A:505–13.
- [30] Vasel CH, Krawitz AD, Drake EF, Kenik EA. Binder deformation in WC-(Co, Ni) cemented carbide composites. *Metal Mater Trans A* 1985;16A:2309–17.
- [31] Erling G, Kursawe S, Luyck S, Sockel HG. Stable and unstable fracture surface features in WC-Co. *J Mater Sci Lett* 2000;19:437–8.
- [32] Roebuck B, Mingard KP, Nordenstrom H, Halling E. Compression fatigue damage in hardmetals. In: Sigl LS, Rödhammer P, Wildner H, editors. *Proceedings 17th Plansee Seminar, 3. Reutte, Austria: Plansee Group; 2009 [AT 9/1-13]*

- [33] Tarragó JM, Jiménez-Piqué E, Turón M, Rivero L, Schneider L, Llanes L. Toughening and fatigue micromechanisms in hardmetals: FESEM/FIB tomography characterization. In: Sigl LS, Kestler H, Wagner J, editors. Proceedings 18th Plansee Seminar. Reutte, Austria: Plansee SE; 2013 [HM54/1-9]

List of figures

Figure 1. Hardness (left) and fracture toughness (right) values for studied materials.

Figure 2. Determined crack growth rates (da/dN) plotted against ΔK (top) and K_{max} (bottom) for the investigated cobalt binder grades with medium (left) and high (right) binder content determined at two different load ratios of 0.1 and 0.5.

Figure 3. Determined crack growth rates (da/dN) plotted against ΔK (top) and K_{max} (bottom) for investigated CoNi binder grades with medium (left) and high (right) binder content determined at two different load ratios of 0.1 and 0.5.

Figure 4. Fatigue crack growth path for the investigated 15CoC cemented carbide.

Figure 5. Fatigue threshold as a function of the mean grain size for the cemented grades investigated by Llanes et al. [15], Coureaux [21] and Torres et al. [26] together with the hardmetals here studied.

Figure 6. Geometric characterization of the fatigue crack growth path.

Figure 7. Weighted mean deflected angle (left) and linear roughness (right) for the studied materials.

Figure 8. Up-and-down fatigue tests used to determine mean fatigue limit for the (a) 11CoM, (b) 10CoC, (c) 15CoC and (d) 15CoNiC here studied cemented carbides.

Figure 9. Example of a microstructure heterogeneity acting as an initial point for fatigue crack growth. Fatigue crystallographic features are observed in the vicinity of the starting critical flaw.

Figure 10. Fatigue sensitivity as a function of binder mean free path for the hardmetals here studied. The trends described by Llanes et al. [15] for WC-Co is also presented (dashed lines) [15]. For $R=0.1$ the trend described by Llanes is updated with the results obtained in this investigation (full red line).

Figure 11. Scanning electron micrographs corresponding to stable crack growth under cyclic loads ($R=0.1$) for the 15CoC and 15CoNiC investigated hardmetals. Fatigue facets are neatly discerned in the metallic constitutive phase.

List of tables

Table 1. Microstructural parameters for the studied hardmetal grades.

Table 2. Hardness, strength parameters and fracture toughness for the investigated hardmetal grades.

Table 3. FCG threshold (K_{th}) and fatigue sensitivity [$1-(K_{th}/K_{Ic})$] for the studied hardmetal grades.

Table 4. Estimated and experimentally determined fatigue limit, in terms of maximum applied stress, for four hardmetal grades studied.

Table 1. Microstructural parameters for the studied hardmetal grades.

Grade	%wt. binder	d_{WC} (μm)	C_{WC}	λ_{binder} (μm)
11CoM	11%Co	1.12 ± 0.71	0.38 ± 0.07	0.42 ± 0.28
10CoC	10%Co	2.33 ± 1.38	0.31 ± 0.11	0.68 ± 0.48
15CoM	15%Co	1.15 ± 0.92	0.30 ± 0.07	0.55 ± 0.46
15CoC	15%Co	1.70 ± 1.08	0.27 ± 0.07	0.77 ± 0.54
10CoNiM	8%Co-2%Ni	1.04 ± 0.83	0.41 ± 0.08	0.36 ± 0.29
10CoNiC	8%Co-2%Ni	1.44 ± 0.86	0.38 ± 0.08	0.47 ± 0.30
15CoNiM	12%Co-3%Ni	1.26 ± 0.81	0.29 ± 0.06	0.60 ± 0.40
15CoNiC	12%Co-3%Ni	1.50 ± 1.00	0.28 ± 0.07	0.68 ± 0.49

Table 2. Hardness, strength parameters and fracture toughness for the investigated hardmetal grades.

Grade	HV30 (GPa)	σ_r (MPa)	Weibull modulus	K_{Ic} (MPa\sqrt{m})
11CoM	12.8 \pm 0.2	3101 \pm 102	36	13.9 \pm 0.3
10CoC	11.4 \pm 0.2	2489 \pm 85	35	15.8 \pm 0.3
15CoM	11.2 \pm 0.1	2912 \pm 88	39	15.2 \pm 0.4
15CoC	10.2 \pm 0.1	2570 \pm 54	54	17.0 \pm 0.2
10CoNiM	12.3 \pm 0.1	2720 \pm 198	23	14.2 \pm 0.4
10CoNiC	11.6 \pm 0.1	2534 \pm 94	32	15.3 \pm 0.3
15CoNiM	10.2 \pm 0.1	2634 \pm 101	33	15.8 \pm 0.4
15CoNiC	9.45 \pm 0.1	2716 \pm 101	31	17.3 \pm 0.4

Table 3. FCG threshold (K_{th}) and fatigue sensitivity [$1-(K_{th}/K_{Ic})$] for the studied hardmetal grades.

Grade	K_{th} (MPa√m)		$1-K_{th}/K_{Ic}$	
	R=0.1	R=0.5	R=0.1	R=0.5
11CoM	7.6 ± 0.1	8.6 ± 0.2	0.45 ± 0.01	0.38 ± 0.02
10CoC	8.3 ± 0.1	10.4 ± 0.2	0.47 ± 0.01	0.34 ± 0.02
15CoM	7.6 ± 0.1	9.1 ± 0.1	0.50 ± 0.01	0.40 ± 0.02
15CoC	8.5 ± 0.2	9.6 ± 0.2	0.50 ± 0.01	0.44 ± 0.01
10CoNiM	7.8 ± 0.2	9.0 ± 0.1	0.45 ± 0.02	0.37 ± 0.02
10CoNiC	8.0 ± 0.1	9.7 ± 0.1	0.48 ± 0.01	0.37 ± 0.01
15CoNiM	7.7 ± 0.1	9.6 ± 0.2	0.51 ± 0.01	0.39 ± 0.02
15CoNiC	7.9 ± 0.2	9.8 ± 0.1	0.54 ± 0.02	0.43 ± 0.01

Table 4. Estimated and experimentally determined fatigue limit, in terms of maximum applied stress, for four hardmetal grades studied.

Grade	Estimated fatigue limit (MPa)	Experimentally determined fatigue limit (MPa)
11CoM	1696 ± 70	1603 ± 97
10CoC	1308 ± 53	1250 ± 84
15CoC	1390 ± 61	1285 ± 43
15CoNiC	1244 ± 91	1240 ± 63

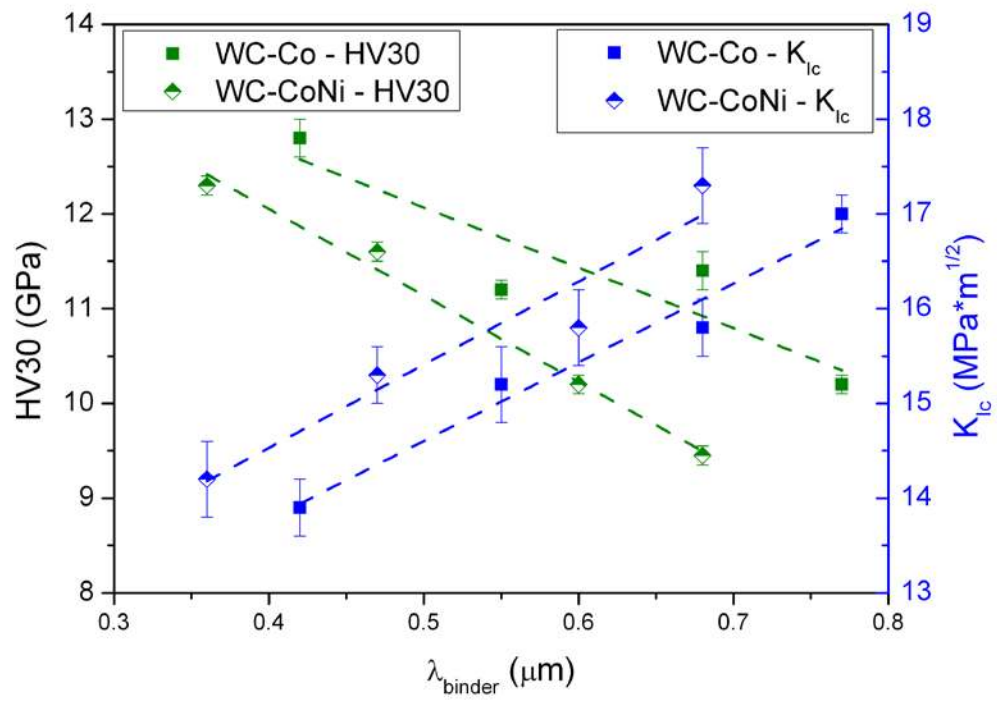


Figure 1. Hardness (left) and fracture toughness (right) values for studied materials.

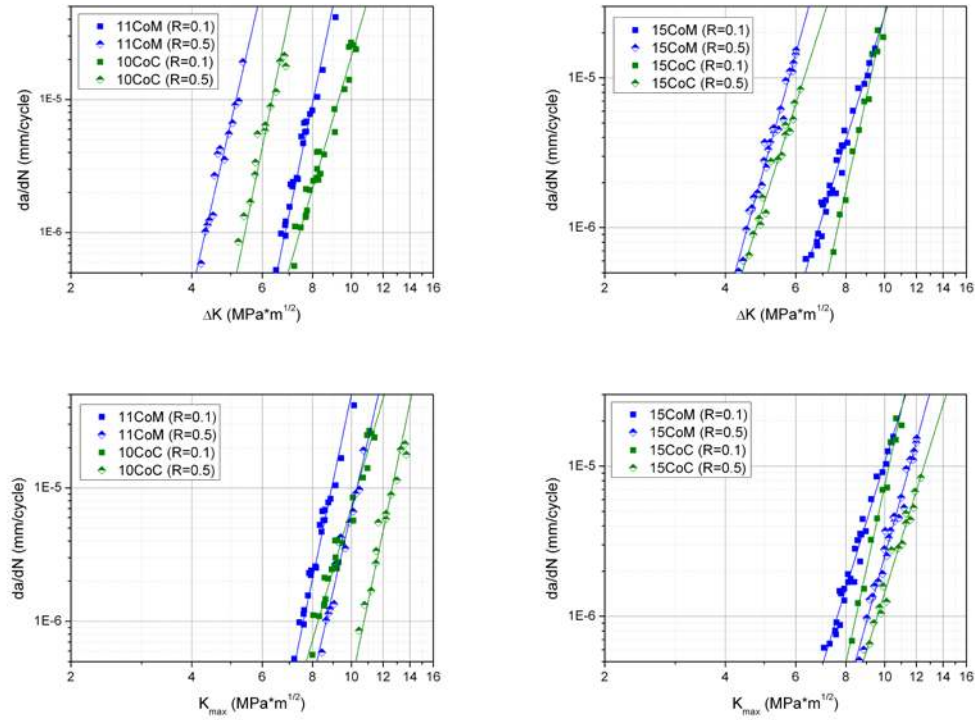


Figure 2. Determined crack growth rates (da/dN) plotted against ΔK (top) and K_{\max} (bottom) for the investigated cobalt binder grades with medium (left) and high (right) binder content determined at two different load ratios of 0.1 and 0.5.

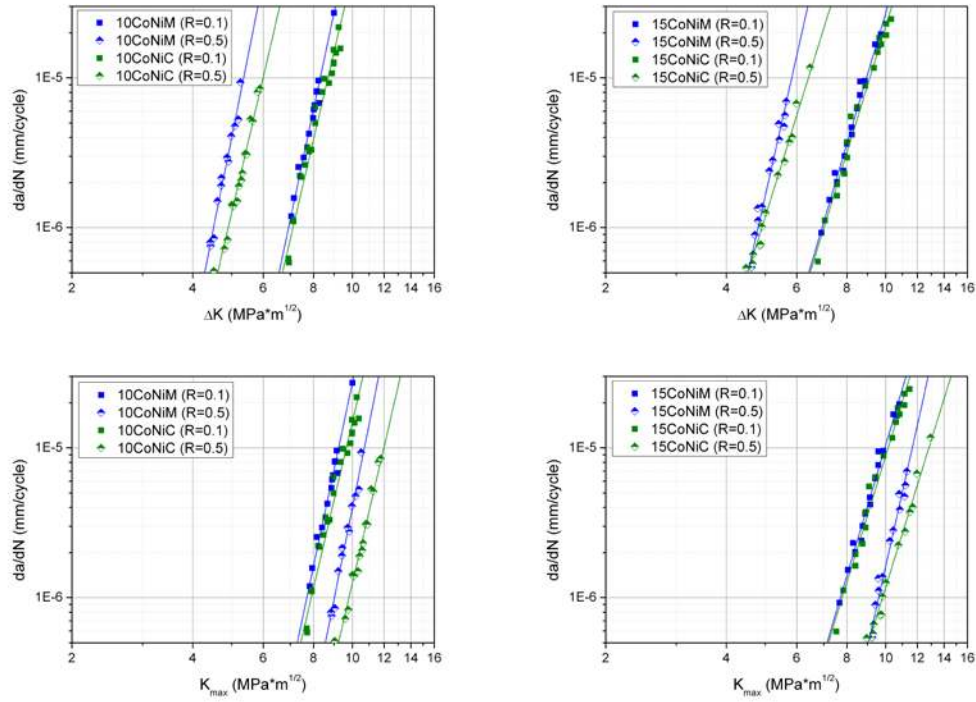


Figure 3. Determined crack growth rates (da/dN) plotted against ΔK (top) and K_{\max} (bottom) for investigated CoNi binder grades with medium (left) and high (right) binder content determined at two different load ratios of 0.1 and 0.5.

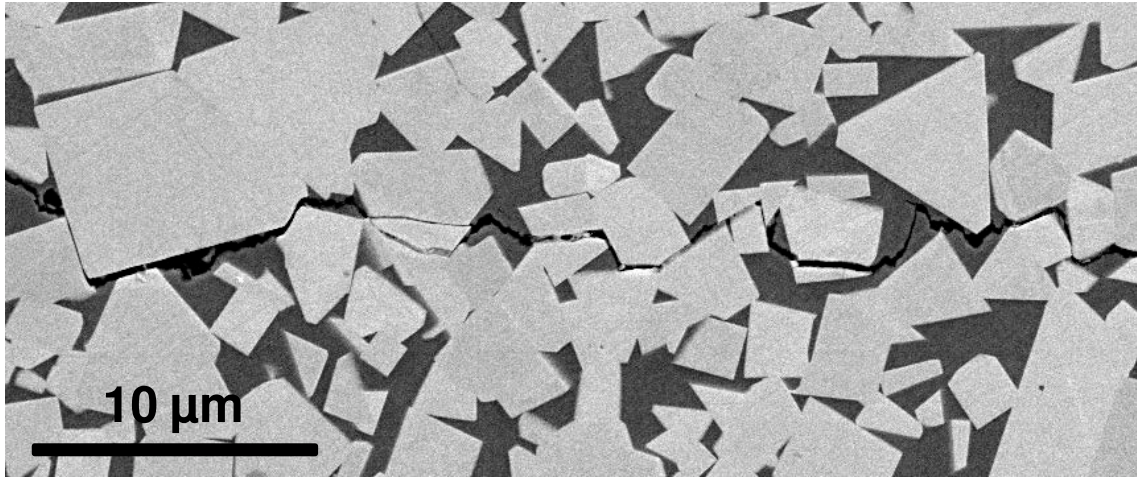


Figure 4. Fatigue crack growth path for the investigated 15CoC cemented carbide.

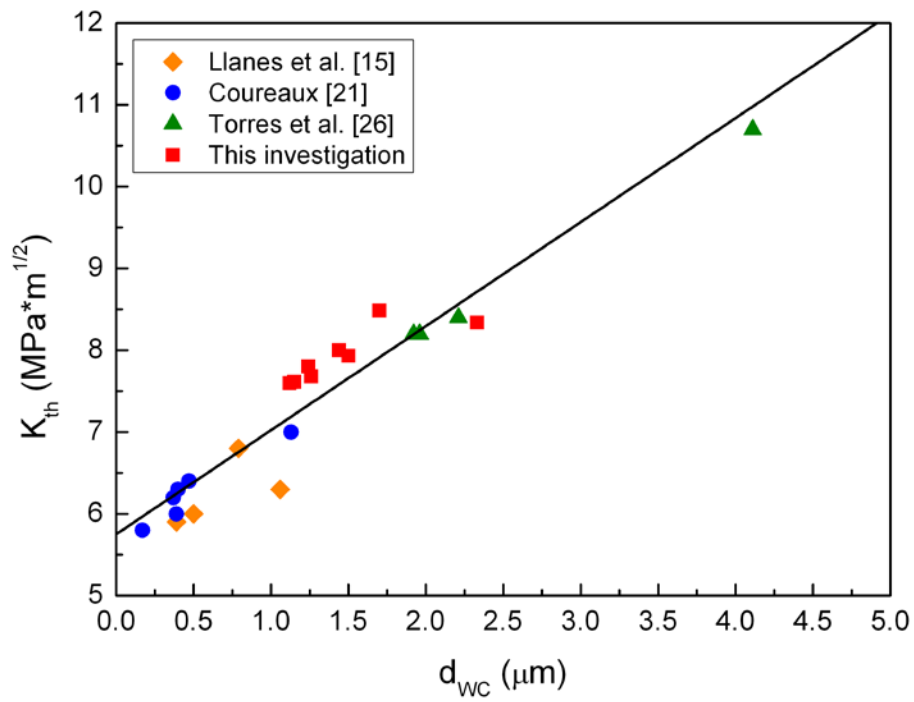


Figure 5. Fatigue threshold as a function of the mean grain size for the cemented grades investigated by Llanes et al. [15], Coureaux [21] and Torres et al. [26] together with the hardmetals here studied.

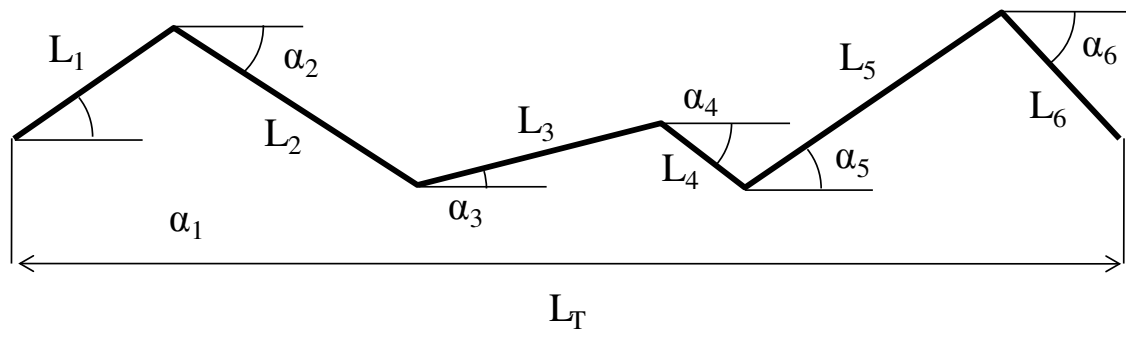


Figure 6. Geometric characterization of the fatigue crack growth path.

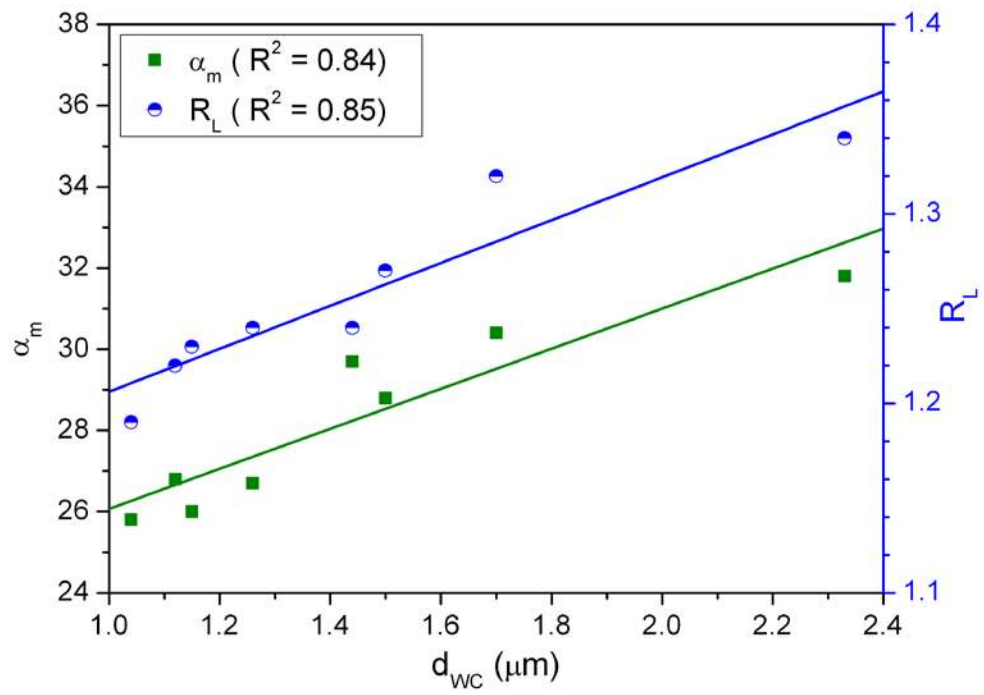


Figure 7. Weighted mean deflected angle (left) and linear roughness (right) for the studied materials.

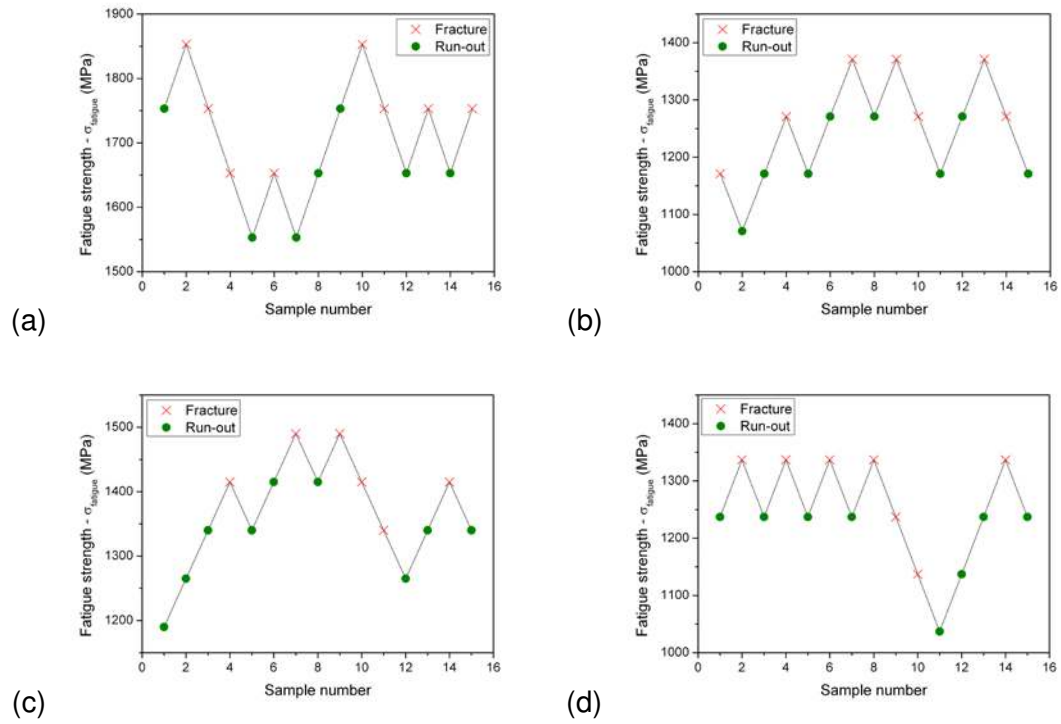


Figure 8. Up-and-down fatigue tests used to determine mean fatigue limit for the (a) 11CoM, (b) 10CoC, (c) 15CoC and (d) 15CoNiC here studied cemented carbides.

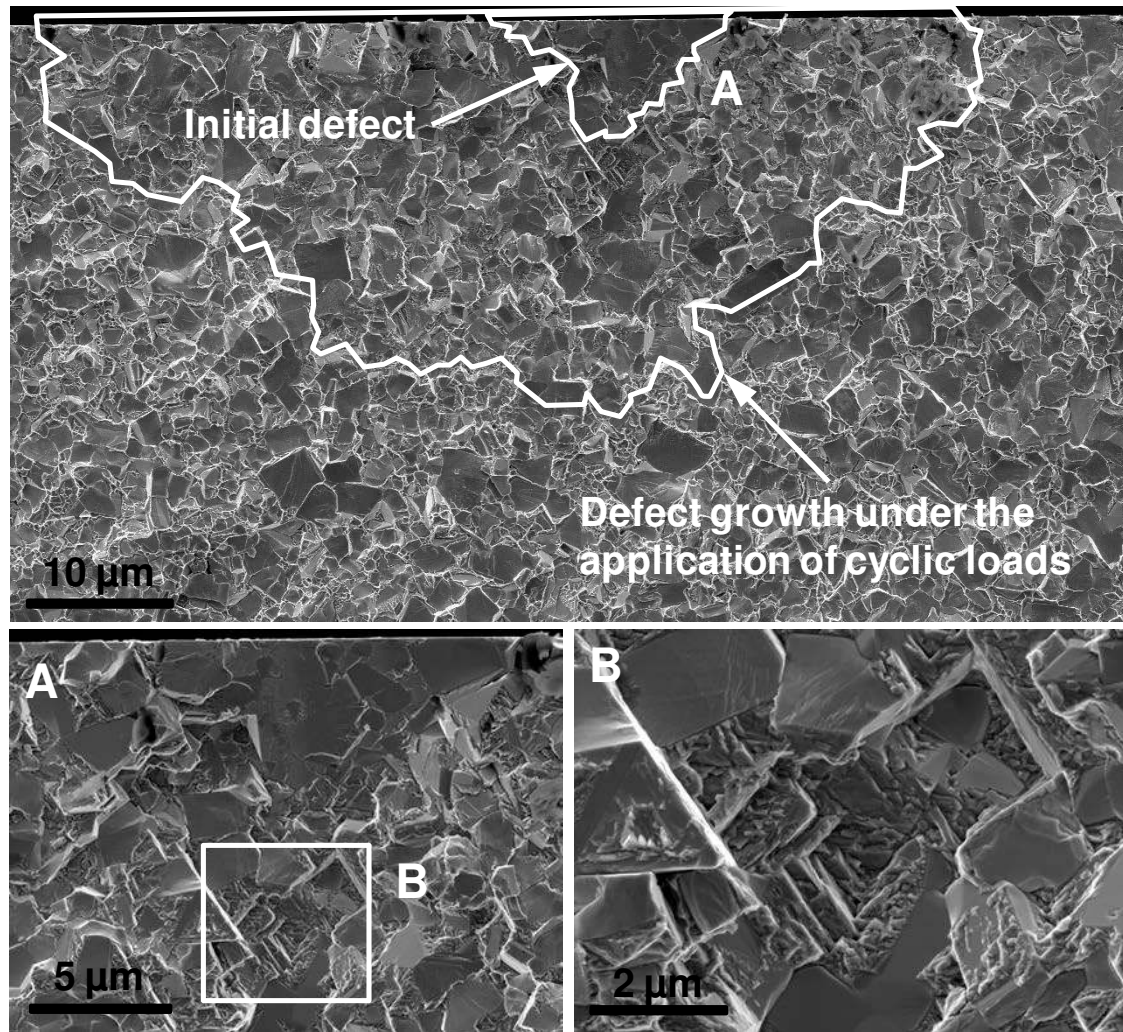


Figure 9. Example of a microstructure heterogeneity acting as an initial point for fatigue crack growth. Fatigue crystallographic features are observed in the vicinity of the starting critical flaw.

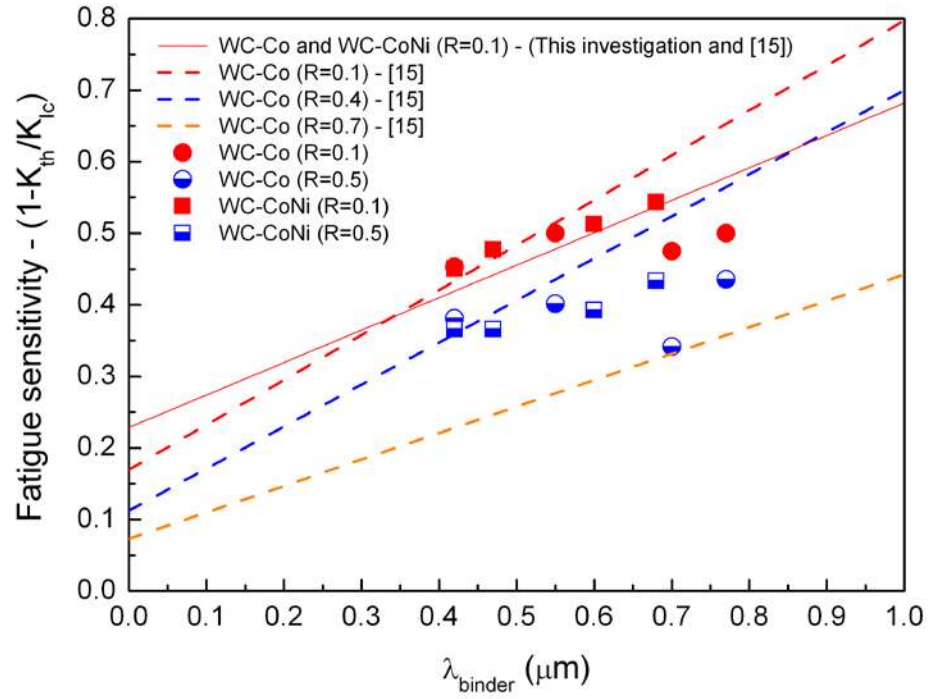


Figure 10. Fatigue sensitivity as a function of binder mean free path for the hardmetals here studied. The trends described by Llanes et al. [15] for WC-Co is also presented (dashed lines) [15]. For R=0.1 the trend described by Llanes is updates with the results obtained in this investigation (full red line).

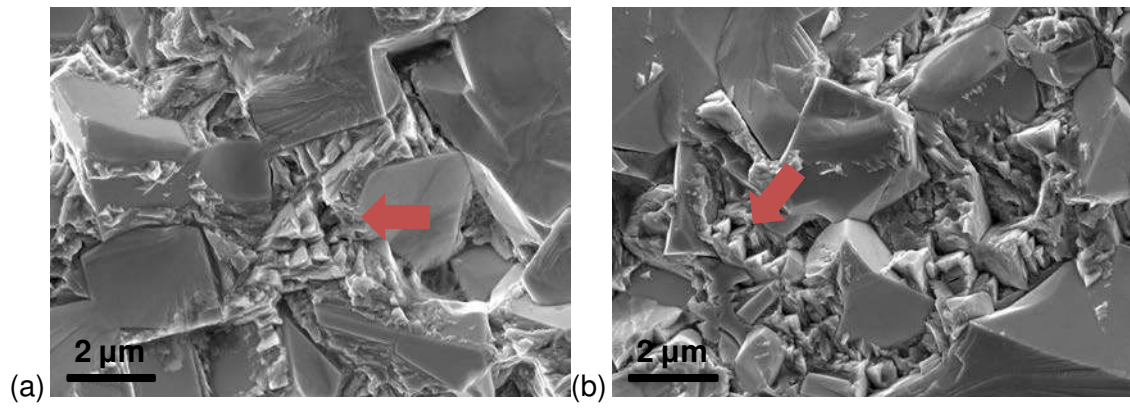


Figure 11. Scanning electron micrographs corresponding to stable crack growth under cyclic loads ($R=0.1$) for the 15CoC and 15CoNiC investigated hardmetals. Fatigue facets are neatly discerned in the metallic constitutive phase.